Evidence for local moment formation around a positive muon in graphite

J. A. Chakhalian, R. F. Kiefl, S. R. Dunsiger, W. A. MacFarlane, and R. Miller
Department of Physics and Astronomy, UBC, Vancouver, British Columbia, Canada V6T 1Z1

J. E. Sonier
Department of Physics, Simon Fraser University, Burnaby, British Columbia, Canada V5A 1S6

J. E. Fischer
Materials Science Department and Laboratory for the Structure of Matter, University of Pennsylvania, Philadelphia, Pennsylvania 19104-6272

(Received 10 January 2002; revised manuscript received 3 July 2002; published 17 October 2002)

The local-electronic structure of the positive muon has been investigated in the semimetal graphite using muon spin rotation/relaxation. Both the muon Knight shift and spin-relaxation rate in highly oriented pyrolytic graphite are anomalously large compared to simple metals and both have an unusual temperature dependence. These results indicate that a local moment forms around the muon due to the low carrier density. In contrast, measurements on metallic LiC_6 reveal a smaller muon Knight shift, which is opposite in sign (negative) and almost temperature independent. We suggest this is due to the core polarization of a Mu^-Li^+ complex.

DOI: 10.1103/PhysRevB.66.155107 PACS number(s): 71.55.Ak, 75.20.Hr, 72.10.Fk, 75.30.Hx

I. INTRODUCTION

The electronic and magnetic properties of an isolated positively charged impurity in a degenerate electron gas have been the subject of numerous theoretical studies because of their fundamental importance. Several independent techniques, including cluster calculations,[1,2] local-density calculations based on the Kohn-Sham formalism,[3–6] and jellium model calculations,[7,8] have revealed the existence of a doubly occupied bound state for a wide range of metallic densities starting with $r_s > 1.9$ a.u. The theoretically predicted bound state is very shallow, the deepest being for $r_s \approx 4$ a.u. In principle, one could test such theories experimentally by carrying out nuclear magnetic resonance (NMR) on isolated hydrogen in conductors with different carrier concentrations. However, it is not always possible to dissolve hydrogen into a given conductor. Furthermore, the concentration of hydrogen needed for NMR (10^{19} cm^{-3}) is, in general, too high to guarantee isolation from other hydrogen atoms and/or residual impurities.

Alternatively, one can deduce information on isolated hydrogen using the technique of muon spin rotation (μSR), in which the positive muon is implanted into the material of interest. The muon (μ^+) is an elementary particle, which is closely related to the electron from a particle physics point of view, since like the electron it has no discernible structure. However, the electronic structure around the positive muon in a solid is virtually identical to that of hydrogen, because the muon mass, although only (1/9)th that of a proton, is still much more than that of the electron. For example, the reduced electron mass for a muonium atom (μ^+e^-) in vacuum is almost equal to that of a hydrogen atom. Muons typically occupy interstitial lattice sites and are studied in the infinitely dilute limit—one muon in the sample at a time. Also because of the short muon lifetime, 2.2 μs, they are typically isolated from residual impurities in the sample. For these reasons muon implantation is an excellent way to simulate the behavior of an isolated hydrogenic impurity.

These aspects of the muon have been used extensively in semiconductors, where the muon and its associated paramagnetic centers provide indirect information on isolated hydrogen, which itself is a difficult impurity to isolate and study with conventional methods.[9] In intrinsic semiconductors, muonium centers exhibit hyperfine interactions between the unpaired electron and the muon spin, which can be used to characterize the local electronic structure. In fact almost all the information on isolated hydrogen in semiconductors comes indirectly through work on muonium. Studies confirm that the electronic structure of muonium is virtualy identical to that of isolated hydrogen in the few cases where both muonium and hydrogen can be studied. On the other hand, the dynamics for the muon can be very different from hydrogen due to the much lighter mass of the muon.

It is not as easy to obtain equivalent information on muonium in conductive materials where the unpaired electron spin, bound to the muon, interacts strongly with the conduction electrons. In fact it can be difficult to even verify that a local electronic moment exists in a metallic environment. This is because the large *static* hyperfine fields which typify muonium in nonconductors are generally absent in conductors. Instead the strong exchange interaction between the bound electron on the muon and electrons in the conduction band is expected to mask any obvious signature of muonium. Nevertheless the presence of such a moment should produce detectable residual effects. For example, if a paramagnetic muoniumlike state exists in a simple metal, it should behave as a Kondo impurity[10–12] and will have a characteristic temperature-dependent local spin susceptibility. In this case the muon Knight shift should be very large and temperature independent below the Kondo temperature (T_K), where the moment is effectively screened by the conduction electrons. At higher temperatures where the screening cloud is shaken off, the Knight shift should fall as $1/(T+T_K)$. It is interesting to note that in the strong-coupling limit of the Kondo

model, a muoniumlike state would bind a second electron in the spin singlet state analogous to the Mu^- ion[13] (see below). This may be related to the ground state predicted from density-functional theory for a single positive charge in an electron gas.[4,5] In addition to a large Knight shift, one might also expect the muon induced bound state in a metal to exhibit an unusually large muon spin relaxation (Korringa relaxation) due to the large hyperfine interaction between the muon and the quasibound electron. This acts to amplify the muon spin flip scattering with electrons at the Fermi surface.[14]

Empirically, the carrier density and *location* of the muon in the lattice are important factors in determining the behavior of a local moment around the muon in a conductor.[15] For example, in metallic alkali-metal doped fullerides, a vacuumlike muonium atom (μ^+e^-) is stable on the inside of the C_{60} cage. This is evidenced by the characteristic field-dependent spin-relaxation rate of muonium undergoing rapid spin exchange with conduction electrons at the Fermi surface.[16] The interaction of this local moment with the conduction electrons is very weak, likely due to the low electron density inside the C_{60} cage. In other words, the Kondo temperature is negligibly small and no appreciable screening of the moment is seen. On the other hand, muons on the outside of the C_{60} cage do not show any evidence for a local moment. It seems likely that a spin singlet state such as Mu^- is formed for this muon site(s). Such a state may be considered a Kondo impurity, but in the strong-coupling limit where the electronic moment is heavily screened. Recently, paramagnetic muonium has also been identified[17] in heavily doped *n*-type Si with a carrier concentration in the range $\sim 10^{19}$ cm^{-3}. The magnitude and temperature dependence of the local spin susceptibility are clear signatures of the same bond-centered muonium seen in intrinsic Si. Furthermore, the simple Curie-like local susceptibility indicates that the Kondo temperature in very small and thus one is in the weak-coupling limit. It is interesting to note that the muon-electron hyperfine interaction in a heavily doped *n*-type material is reduced compared to the same center in intrinsic Si, implying that the electronic structure depends on the carrier concentrations. A signal with no appreciable frequency shift was also observed in this experiment, which is attributed to the Mu^- ion at the tetrahedral interstitial site. Theoretically this is the predicted stable charge state for muonium/hydrogen in *n*-type silicon. One can interpret the results on doped C_{60} and *n*-type silicon as follows: Depending on the muon site, the Kondo coupling constant shifts between the two extremes—very weak to very strong. More specifically for muons at the center of the C_{60} cage or muons at the center of the Si-Si bond, one is in the weak-coupling limit and thus the full moment is seen down to very low temperatures. This can be understood from a local structural point of view, since it may be energetically unfavorable for the muonium atom to bind a second electron due to the strong on-site Coulomb repulsion. One the other hand, if the muon is at a site where the on-site Coulomb repulsion is not too strong, then muonium can bind a second electron (e.g., Mu^-) which is a spin singlet. Under these circumstances the moment is screened until the singlet state is ionized. This would correspond to the strong-coupling limit of the Kondo model.[13]

In normal metals, where the electron density is much higher (10^{22} cm^{-3}), no clear evidence of a moment on the muon can be found.[15] For example, in silver the muon Knight shift is small, positive ($+94$ ppm), and temperature independent, such as the Pauli spin susceptibility. In a conventional picture the screening cloud of conduction electrons reduces the muon Coulomb potential to the extent that no bound state is formed.[18] At lower densities the muon may form a spin singlet (e.g., something like the Mu^- ion in which the muon might bind two electrons in a $1s$-like orbit).[5] In the Kondo picture one is in the strong-coupling limit. The observed Knight shift is then attributed to a small overlap of the polarized conduction-electron states at the Fermi surface with the muon. However, this bound state is in the conduction band and therefore should be regarded as a broad *resonance*. Also note that despite the short screening radii in metals (typically $<1-2$ Å), an extra electron attached to this shallow bound state is screened by the long-wavelength electrons from the bottom of the conduction band. Because of this, the predicted shallow state is rather extended (~ 10 Å) and broadened even further by the collisions with itinerant electrons. This ill-defined nature of the bound state and an overlap of the screening cloud with the neighboring ions make the task of direct experimental identification of this state difficult or impossible.[15] Another possibility is that the covalent bonding electronic structures (i.e., Mu-metal) similar to the observed hydrogen induced VH_x and PdH_x states[19–21] may also exist in metals.

Semimetals lie in an intermediate region between a doped semiconductor, where localized bound states of the muon clearly exist, and good metals, where no such moments are apparent. Although semimetals have a carrier concentration typical of a heavily doped semiconductor, at low temperatures they have a well-defined Fermi surface. For example, at low temperatures they exhibit de Haas–van Alphen (dHvA) oscillations in the magnetic susceptibility from Landau levels crossing the Fermi surface. On the other hand, at relatively moderate temperatures (above 50 K) they cannot be considered a degenerate electron gas since k_BT becomes comparable to the small Fermi energy. Indeed in the semimetal antimony the muon Knight shift is anomalously large at low temperatures[22] and has a temperature dependence which follows qualitatively what one expects for a simple Kondo impurity up until about 100 K.[23] On the other hand, one needs to mention that the muon behavior in semimetals is far from being understood; for example, the μSR measurements on semimetallic Bi and As produced no unusually large Knight shift.[24] This clearly indicates that the density of carriers alone cannot account for the mechanism of bound-state formation, and further μSR measurements on semimetals are certainly required.

Graphite is another interesting semimetal and the focus of the present study. It is highly two-dimensional, has a small free-carrier concentration equal to $n_c = 3\times 10^{18}$ cm^{-3} and a correspondingly narrow conduction-band width (~ 0.023 eV). One can anticipate that the muon is significantly underscreened in such a material compared to a

simple metal, since the mean distance between carriers is very large ($2r_s \sim 81$ a.u.). For example, the Thomas-Fermi wave vector k_o in graphite is only 0.34 $Å^{-1}$, which is several times smaller than in normal metals. Graphite also has historic significance since it was the first material on which muon spin rotation was performed to confirm parity violation in weak interactions.[25] However, very little work has been done on it since that time. It is known that the Knight shift at room temperature is unusually large.[26] There has also been a recent study[27] of the spin-relaxation state at high temperatures, which we discuss later. Additional scientific motivation for understanding the behavior of hydrogen in graphite is that related compounds are used as a negative electrode in lithium batteries. For example, it has been reported[28,29] that there is a strong correlation between lithium capacity and the content of hydrogen in graphitic compounds.

In this paper, we present detailed measurements of the muon Knight shift and spin-relaxation rate in highly oriented pyrolytic graphite (HOPG) over a wide range of temperatures. Both the Knight shift and spin-relaxation rate are anomalously large compared to what one would expect from the small Pauli susceptibility. Furthermore, there is a large isotropic component to the Knight shift. These results are strong evidence for the existence of a local electronic moment on or near the muon. Surprisingly, the Knight shift *increases* with temperature up to about 500 K, which indicates there is a significant transfer of spin density to the muon at elevated temperatures.

In addition, we have performed μSR measurements on stage-1 lithium intercalated graphite. In this metallic compound the Knight shift is much smaller and opposite in sign (negative), indicating that the local electronic structure for the muon is dramatically different than in pure graphite. We suggest that the much higher Fermi energy favors the formation of a diamagnetic Mu^- state.

II. EXPERIMENTAL

All measurements have been performed on the M20 or M15 beam lines at TRIUMF, which provide a beam of nearly 100% spin polarized positive surface muons with a mean momentum of 28 MeV/c. The spin polarization was rotated perpendicular to the axis of the superconducting solenoid and muon beam direction. The samples were cut from high-purity HOPG with the $\vec{c}$ axis aligned to better than 2°. A single piece or five pieces were used, depending on whether the field was applied in parallel or perpendicular to the average $\vec{c}$ direction, respectively. The magnitude of the applied magnetic field was chosen to be 1.45 T in order to attain the most accurate Knight shift. Although the frequency shift scales with the magnetic field, the amplitude of the μSR signal decreases at higher fields when the period of the Larmor precession frequency becomes comparable to the timing resolution of the detectors.

In order to make precise Knight-shift measurements, we developed a μSR technique which allows us to collect the data on a sample and a reference simultaneously.[30] Figure 1 shows a schematic of the apparatus used for frequency measurements below RT. The helium flow cryostat has been

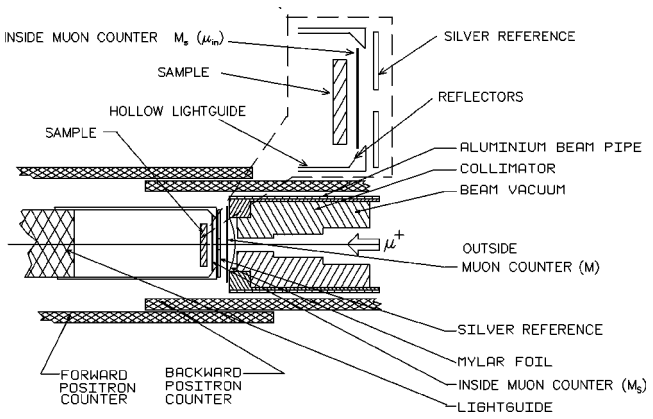

FIG. 1. Schematic of the apparatus for precise measuring of two μSR spectra simultaneously.

omitted for the purpose of clarity. The collimated muon beam passes through a thin plastic scintillator (M) before entering the cryostat. The crucial element of our setup is the second thin muon counter (M_s) in the sample space of the cryostat. Light from the edges of the M_s counter is reflected down the axis of a hollow light guide (covered with silverized mylar) and out the back end of the cryostat to a photomultiplier (not shown). The M_s scintillator is tightly sandwiched between the sample on the downstream and the reference just upstream. The reference is an annular disk of high-purity silver foil (99.99%) with a 1-cm-diameter hole at the center. About half of the incoming muons stop in the reference without triggering M_s, while half pass through the hole, trigger the M_s counter, and then stop in the sample. This allows us to distinguish muons stopping in the sample from those stopping in the reference.

Such a detector arrangement has several advantages. Most importantly, it allows us to collect μSR spectra on the reference and the sample simultaneously, thus eliminating many of the systematic effects (e.g., drift in an external magnetic field, thermal contraction, instabilities in electronics, changes in the beam properties, etc.). Second, the sample spectra are exceptionally clean and have no detectable signal from the reference or elsewhere. This eliminates other errors due to the variations in the background to foreground ratio which can influence the frequency measurement. Note that in general, the background and foreground signals are very close in frequency and are thus not easily distinguished. The statistical accuracy on individual frequencies is about 2 ppm after about an hour of data collection ($\sim 10^7$ events) and the systematic error on the frequency shift is estimated to be at about the same level.

A similar geometry was used for measurements above room temperature. However in this case, the second muon counter and silver mask were placed just outside the oven and 20 mm in front of the sample. This was necessary since it is not possible to use a plastic scintillator at high temperatures.

III. GRAPHITE RESULTS

Figure 2 shows the temperature dependence of the measured Knight shift with respect to the silver reference mea-

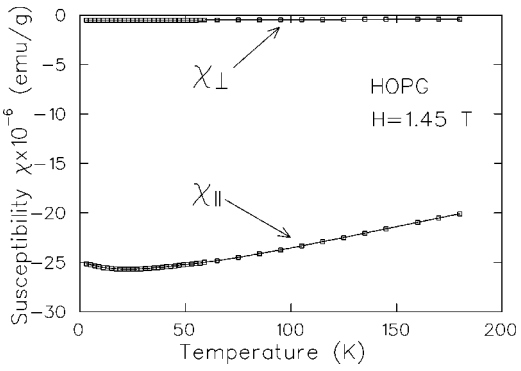

FIG. 2. Temperature dependence of the magnetic dc susceptibility of HOPG in an applied magnetic field of 1.45 T measured with **H** parallel and perpendicular to the *c* axis of graphite.

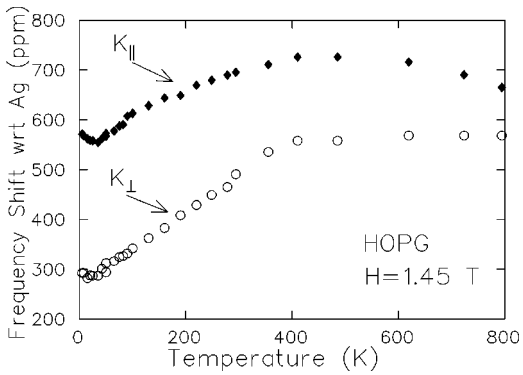

FIG. 3. Shift in muon precession frequency in HOPG relative to Ag as a function of temperature in an applied magnetic field of 1.45 T.

sured with the magnetic field parallel and perpendicular to the $\vec{c}$ axis of HOPG. The magnitude of the Knight shift in the sample without correcting for bulk magnetization is defined according to the following formula:

$$K_s=(B_s-H)/H, \tag{1}$$

where B_s is the total magnetic field at the muon site in the sample and H is the external applied field. Subtracting the known Knight shift of the reference (K_r) from both sides, one obtains the Knight shift in the sample in terms of the measured or known quantities:

$$K_s-K_r=(B_s-B_r)/H \tag{2}$$

$$=(f_s-f_r)/\gamma_\mu H \tag{3}$$

$$\cong(f_s-f_r)/f_r, \tag{4}$$

where $f_s=\gamma_\mu B_s$ is the observed muon precession frequency in the sample, f_r is the muon precession frequency in the reference, K_r is the known Knight shift in the reference (94 ppm), and where we approximate $\gamma_\mu H$ by f_r.

Several corrections to this formula are needed. First the external field at the reference and sample positions are not identical. This shift was determined to be about 7 ppm by mounting a second piece of silver at the sample position. Also, we are interested in the induced frequency shift due to the hyperfine interaction with the electrons ($B_{\rm hf}$), whereas the total magnetic B_s field in Eq. (1) has other contributing terms originating from the bulk magnetization of the sample:[31]

$$B_s=H+B_{\rm hf}+B_{\rm dem}+B_L+B_{\rm dip}, \tag{5}$$

where H is the applied magnetic field, $B_{\rm dem}$ is the demagnetization field, B_L is the Lorentz field, and $B_{\rm dip}$ is the dipolar field from moments within the fictitious Lorentz sphere surrounding the muon. $B_{\rm dem}$ and B_L are the macroscopic contributions to the magnetic field and can be evaluated as follows:

$$B_{\rm dem}=-NM, \quad B_L=\frac{4\pi}{3}M, \quad M=\chi H, \tag{6}$$

where N is the geometry-dependent demagnetization factor, M is the bulk magnetization, and χ is the total magnetic susceptibility of the sample. The dipolar field ($B_{\rm dip}$) can be evaluated numerically as a sum of $\Sigma_i b_i(\vec{r}_\mu-\vec{r}_i)$ over the individual carbon atoms inside a Lorentz sphere of a sufficiently large radius. This term is opposite in sign to the sum of $B_{\rm dem}$ and B_L and is quite sensitive to the muon site. For example, if one assumes that the muon adopts an interplane equilibrium position, then the overall correction is just a few ppm for $K_\parallel$ and almost zero for $K_\perp$. On the other hand, if the muon was located at a C-H bond length[32] ($\sim$1.19 Å) from a carbon atom, there is a substantial correction for $K_\parallel$ but almost none for $K_\perp$ (see Fig. 2). We suspect that the latter is most likely since the difference between $K_\parallel$ and $K_\perp$ has a temperature dependence close to that of the bulk magnetic susceptibility of graphite. In this case the Knight shift is almost isotropic and has a temperature dependence close to that of $K_\perp$.

A few remarks about the Knight shift data in Fig. 2 are in order. First, the magnitude is anomalously large compared to normal metals considering the small Pauli spin susceptibility in graphite 0.016×10^{-6} emu/g. For example, in a simple metal like Ag the ratio between the Pauli spin susceptibility and the muon Knight shift (+94 ppm) is about 270 times smaller than what is observed in graphite. The parallel Knight shift at 300 K is close to that of a previous measurement on a graphite single crystal[26] if the larger correction is made assuming a C-H bond length (about 250 ppm at RT). Second, the Knight shift has at most a small anisotropy ($K_\parallel/K_\perp\approx2$), in contrast with the bulk magnetic susceptibility where $\chi_\parallel/\chi_\perp\approx49$ (see Fig. 3). Also, the absolute value of the Knight shift steadily increases with temperature (for $T<500$ K), whereas the magnitude of the magnetic susceptibility $\chi_\parallel$ decreases with rising temperature (see Figs. 2 and 3). These observations establish that the local electronic structure around the muon has a much different magnetic response than the conduction electrons of graphite. In particular, the local spin susceptibility at the muon is orders of magnitude larger and far more isotropic than expected from just electrons at the Fermi surface. Lastly, the frequency shift displays an unusual temperature dependence since it *rises* steadily with temperature above from about 20 K up to 500

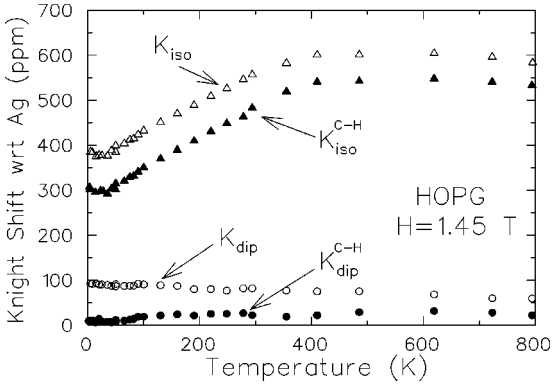

FIG. 4. Temperature dependence of the isotropic $K_{\rm iso}$ and axial or dipolar $K_{\rm dip}$ parts of the muon Knight shift in graphite. The filled circles and triangles represent the corrected value of the Knight shift assuming that a muon is at the C-H bond distance from a carbon atom. The open circles and triangles represent the corrected Knight shift assuming that μ^+ is in the interplane position.

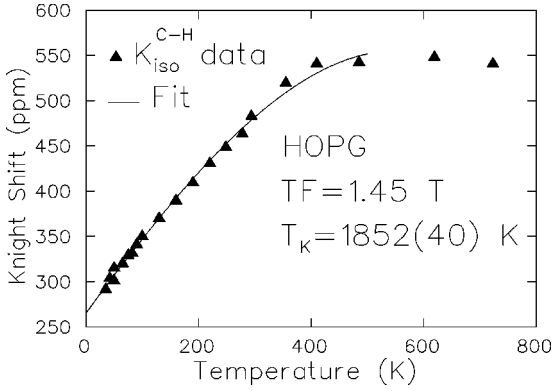

FIG. 5. Temperature dependence of the isotropic $K_{\rm iso}$ part of the Knight shift in graphite. A solid line is the best fit to Eq. (8); the parameters extracted from the fit are given in the main text. The limited dataset between 35 K and 485 K is used to fit the experimental data, which corresponds to the applicable temperature range $T \ll T_K$ for the model.

K. Note there is a slight upturn in $K_{\parallel}$ below 20 K, which we attribute to the influence from the dHvA oscillations, which we discuss below.

This behavior of the Knight shift in graphite is in a marked contrast to that seen in conventional free-electron metals where K_{μ} is temperature independent and proportional to the Pauli spin susceptibility. On the other hand, the observed increase in the Knight shift with temperature is not predicted for a simple Kondo impurity where spin susceptibility is temperature independent below the Kondo temperature and falls like $1/(T+T_K)$ above T_K. Thus although there is good evidence for local moment formation, the temperature dependence suggests that the behavior is more complex than expected from a simple Kondo impurity. In order to elucidate the origin of the unusual temperature dependence of the Knight shift we may calculate the isotropic ($K_{\rm iso}$) and the dipolar ($K_{\rm dip}$) contributions as follows:

$$K_{\rm iso}=\frac{1}{3}(K_{\parallel}+2K_{\perp}), \quad K_{\rm dip}=\frac{1}{3}(K_{\parallel}-K_{\perp}). \tag{7}$$

The linear part of the isotropic Knight shift was fit to the following phenomenological approximation of the Kondo model, which is valid for $T \ll T_K$ and $\mu_B H \ll k_B T$:[33]

$$K_{\rm iso}(T)=J_o\left(\frac{1}{2\pi T_K}-0.433\frac{T^2}{T_K^3}\right), \tag{8}$$

In order to fit the steady rise of $K_{\rm iso}$ with temperature, the Kondo coupling constant J_o is allowed to vary with temperature as $\beta(1+\alpha T)$. The fit gives scaling parameters $\beta=3.0860(4)$, $\alpha=0.0032(4)$ K^{-1} and a Kondo temperature T_K of 1852(40) K (see Fig. 4). Additional evidence for the temperature-dependent coupling $J_o(T)$ comes from $1/T_1$ (see below).

The Korringa-like spin-relaxation rate[34] with the conduction electrons is also anomalous. Normally Korringa relaxation of muon polarization is too slow to be detectable on the μSR time scale. However, if there is a local moment as indicated by the large Knight shift, the muon spin relaxation should be enhanced by the indirect coupling between the muon spin and conduction electrons through the bound electron.[14] This is confirmed by the appreciable muon-spin-relaxation rate at 896 K (see Fig. 5). While $1/T_1$ is close to the detection limit at 295 K (see Fig. 6), it increases steadily at higher temperatures in a nonlinear fashion. Recall that for nuclei in a normal metal, the magnitude of $1/T_1$ is predicted to rise linearly with temperature. The observed relaxation rate rises faster than that predicted from Korringa relaxation (see filled circles in Fig. 6). This breakdown of the Korringa law is attributed to a number of factors, the most important of which is the crossover from degenerate to nondegenerate electron behavior as $k_B T$ exceeds about 100 K. In addition, the fact that the Knight shift increases with temperature suggests that the coupling constant $J(T)$ increases with temperature as was indicated by the Knight shift. One can estimate $1/T_1$ in the first Born approximation without the usual assumption of degenerate statistics:

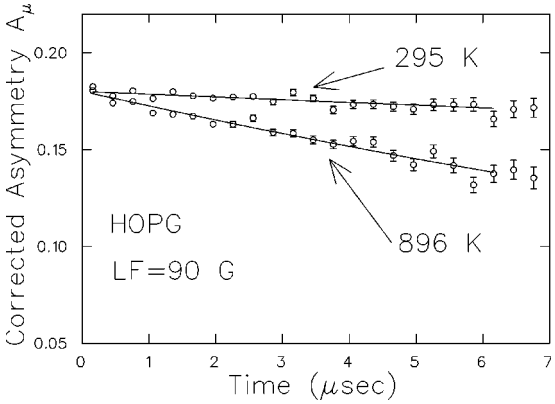

FIG. 6. LF-μSR spectra observed in graphite at $T=295$ K and $T=896$ K. The solid line represents the fit to the exponential relaxation function. The high-temperature data show faster damping. The data are analyzed with a fixed asymmetry and within the first 6 μsecs to avoid a problem with longer time distortions.

$$\lambda \equiv 1/T_1 = J_o^2(T) \int g^2(E) f(E,T)[1-f(E,T)]dE, \quad (9)$$

where $J_o(T)$ is proportional to the coupling constant between the muon and conduction electrons, $g(E)$ is the phenomenological density of states for graphite, and $f(E,T)$ is the Fermi-Dirac distribution with a Fermi energy (chemical potential) fixed at 23 meV. The density of states is estimated as[35]

$$g(E) = 4(0.092/\gamma_o^2)|E - 0.5(\gamma_2 + \Delta) + \text{const}|, \quad (10)$$

where γ_o, γ_2, and Δ (all in eV) are from band-structure theory.[36,37] Equation (9) predicts a nonlinear behavior of $1/T_1$ at high temperature as observed. This can be understood as follows: Recall that the linear behavior in normal metals arises from the fact that only the electrons with $k_B T$ of the Fermi surface participate in the scattering due to Pauli blocking. However at high temperatures in graphite there are two new effects. First, a large fraction of the electrons are already involved in the scattering due to the crossover into nondegenerate statistics. This weakens the temperature dependence. On the other hand, the density of states is strongly energy dependent near the Fermi energy as can be seen from Eq. (10). This causes an increase in the overall number of free carriers available for scattering and a stronger than linear behavior in T. In graphite these two opposing effects compete. The fit of Eq. (9) to a single temperature-independent parameter $J_o = 0.1080(6)$ is shown as a dashed line in Fig. 6. The same model with a temperature-dependent coupling constant $J_o(T) = J_o(1 + \alpha T)$ [$J_o = 1.4125(4)$ and $\alpha = 0.0032(4)$ K^{-1}, where α is the same constant used to fit K_{iso}] reproduces the experimental data rather well (see solid line in Fig. 6).

IV. DISCUSSION ON THE GRAPHITE RESULTS

The results in Fig. 7 show that the isotropic part of the Knight shift dominates and grows with temperature whereas the dipolar part is much smaller and almost temperature independent. Given the evidence for a local moment we adopt a local picture of the center similar to what is used to describe muonium in semiconductors. Then the isotropic part of the Knight shift arises from a contact interaction with a 1*s* hydrogenlike orbital centered on the muon, whereas the dipolar part is attributed to spin density localized on the nearest-neighbor carbon(s).

It should be noted that for muonium substituted free radical or bond-centered muonium in covalent semiconductors [such as GaAs (Ref. 38)], the vast majority of the spin density rests on the neighboring atoms. Thus while the dipolar part of the Knight shift in graphite is much less than the isotropic part, it is possible that most of the magnetic moment is not on the muon but rests on the neighboring carbon atoms. It is interesting to compare this with recent theoretical calculations for muonium interacting with a single graphene plane (see Fig. 8). These calculations predict that the hydrogen/muonium atom bonds to one carbon, with the majority of the spin density on the six neighboring carbons. Of course this is a crude approximation to graphite since the

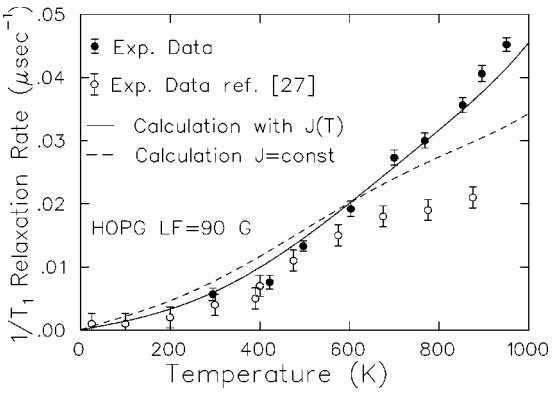

FIG. 7. Temperature dependence of the relaxation rate $1/T_1$ measured at the applied longitudinal field of 90 G in pure graphite above RT. The solid and dashed lines represent our estimates. The difference between our data (solid circles) and the $1/T_1$ result reported in Ref. 27 (empty circles) is not fully understood. One possible difference is in the analysis procedure. In our case the asymmetry of the muon signal has been fixed at all temperatures since the relaxation depends only on the product $A_\mu \lambda$.

muonium would be sandwiched between two graphene layers. Nevertheless, it is likely that a similar structure exists in graphite.

Consider the temperature dependence of K_{iso}, which *increases* between 20 K and 500 K. This is difficult to understand, given that the magnetic susceptibility of any local moment should decrease with temperature. We suggest that the increase in K_{iso} and $1/T_1$ is due to a small temperature induced change in the electronic structure. For example, the contact interaction may increase with temperature as the C-Mu bond length increases. This can be understood since in the limit where the C-Mu bond is broken, the contact interaction on the muon can increase to that of free muonium. Around 500 K the predicted $1/(T + T_K)$ decrease for a Kondo impurity behavior takes over and K_{iso} gradually decreases.

As mentioned previously $K_\parallel$ displays a slight upturn at low temperatures below 20 K. In order to determine the origin of this we measured the bulk magnetic susceptibility in a superconducting quantum interference dervice magnetometer on the same sample of HOPG. The magnetic-field scan data taken at 3 K (see Fig. 9) show very pronounced dHvA oscillations caused by the periodic change in the density of states

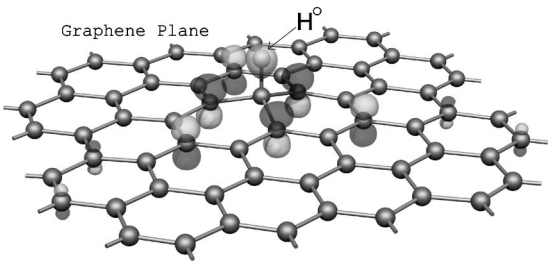

FIG. 8. Molecular-orbital simulation (Ref. 27) on a single sheet of graphite reveals the existence of a loosely bound radical for a hydrogen atom. Note that the spin density is not on a single carbon but rather distributed among nearby carbon atoms.

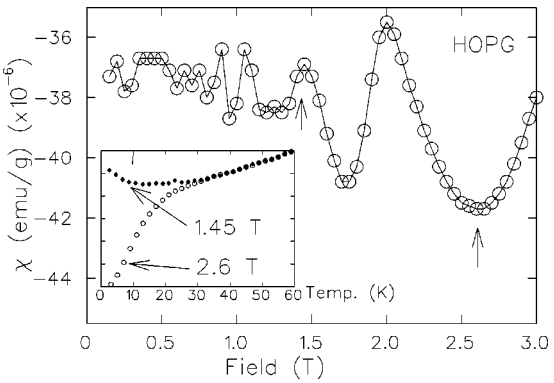

FIG. 9. Oscillations of the magnetic susceptibility in pyrolytic graphite for $H\|c$ and $T=2.4$ K. A magnitude of the applied magnetic field used for the muon Knight-shift measurements is indicated by an arrow. The inset shows the low-temperature part of the magnetic susceptibility in single-crystal graphite with $H\|c$ taken in a magnetic field of 1.45 T and 2.6 T. The apparent change in the shape of the curves follows the de Haas–van Alphen oscillations.

at the Fermi energy brought about by the changing energy spacing between Landau levels. To understand the possible influence of this on the temperature dependence of the Knight shift, we measured the bulk susceptibility as a function of temperature for several applied fields shown as an inset of Fig. 9. As we expected, the low-temperature behavior of the bulk susceptibility depends strongly on the magnetic field. At 1.45 T, where our μSR measurements are performed, the susceptibility shows an upturn at low temperatures whereas at 2.6 T it turns down. This is most likely the explanation for the low-temperature feature seen in $K_{\|}$ (see Fig. 2). Note that the effect is less noticeable for $K_{\perp}$. This confirms our hypothesis that the observed frequency shift for a field parallel to the c axis is strongly influenced by the bulk magnetic susceptibility.

V. LITHIUM INTERCALATED GRAPHITE

For comparison additional μSR measurements were also taken on the lithium intercalated compound LiC_6, which, unlike graphite, is a good metal. LiC_6 belongs to a class of materials in which Li ions form an ordered lattice in between the graphite sheets. Angle-resolved photoemission results[39] show that the Li intercalant is fully ionized with one electron per Li atom transferred to the graphite layers, which leads to the highly increased metallicity. Lithium intercalated compounds are extremely unstable in air and require special handling. In our case the sample of LiC_6 was sealed in a small Al vessel equipped with a thin (50 μm) Kapton window to allow muons to enter the sample.

The muon Knight shift was measured in an external magnetic field of 1.45 T applied along the $\vec{c}$ axis (see Fig. 10). Note that the magnitude of the Knight is about -100 ppm and temperature independent. This is typical for simple metals where the Knight shift tracks the Pauli spin susceptibility.[40] As one might expect, the increased carrier concentration from Li appears to destroy (or completely screen out) the local moment seen in pure graphite. The most

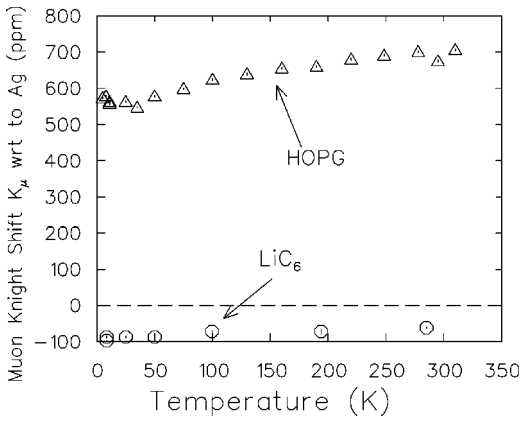

FIG. 10. Temperature dependence of the muon Knight shift in LiC_6. For comparison, the same quantity measured in HOPG is represented by the open circles.

unusual feature in LiC_6 is the sign of the Knight shift (negative) implying that the spin density at the muon site is polarized opposite to the conduction electrons. This suggests that the muon is not in direct contact with the conduction electrons. One possibility is that the increased Fermi level favors the formation of a Mu^- ion, which should bond to the Li^+. We know that the electronic band created by Li^{+}[41] lies above the Fermi level throughout the whole Brillouin zone and is therefore unoccupied. However a local level created by $MuLi^+$ may be below the Fermi surface and leads to a neutral Mu^-Li^+ complex. A similar mechanism has been proposed to explain a hydrogen complex formation in MC_8 (M=K, Rb, and Sc) alkali-metal intercalation compounds.[42] Such a complex may explain the negative Knight shift. For example, the external field polarizes the conduction electrons which are located primarily in the carbon plane. If there is little direct spin density on the MuLi compound, then core polarization of the molecular orbitals for Mu^-Li^+ could lead to a net negative frequency shift. Note that similar core-polarization effects lead to a negative contact interaction for bond-centered muonium in silicon.[43]

In order to investigate the stability of the muon in LiC_6 we have also performed the μSR measurements in zero ap-

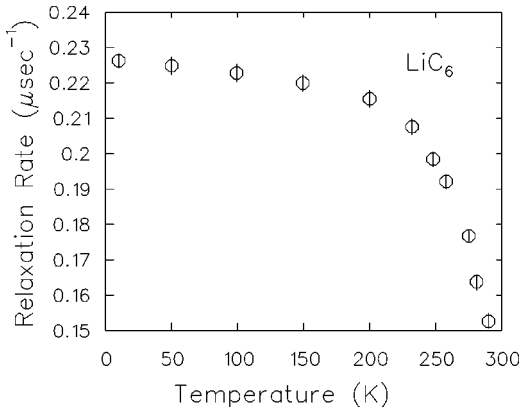

FIG. 11. Zero-field spin-relaxation rate as a function of temperature in LiC_6. At temperatures above 120 K the muon starts hoping and motional narrowing occurs.

plied field (ZF). Figure 11 shows the temperature variation of the muon depolarization rate in ZF, which depends on the strength of the nuclear dipolar interaction with the Li nuclear spins. As seen, the relaxation rate is almost constant below 100 K and then gradually decreases at higher temperatures. The reduction at higher temperatures is attributed to motional narrowing, as the muon hops from one site to the next. These results imply that the muon is stationary on the time scale of a few microseconds below 100 K but begins to move rapidly at higher temperatures. This is a lower limit on where isolated hydrogen will begin to move in LiC_6.

VI. CONCLUSION

In summary, we have studied the local electronic structure for muons implanted in HOPG by means of the muon Knight-shift measurements from 3 K to 900 K. There is an unusually large and temperature-dependent Knight shift, which indicates the formation of a local moment. The isotropic part of the Knight shift is much larger than the dipolar part and rises with temperature. We have interpreted these results in terms of a local model, where the spin density is predominantly on the neighboring carbons and screened heavily at low temperatures. The increase in the isotropic part of the Knight shift, which measures the contact interaction, is in contrast to the conventional temperature dependence for a simple Kondo impurity and indicates that the local structure changes slightly with temperature. In addition, the muon-spin-relaxation rate is large and deviates from the Korringa relation for normal metals. This is likely due to the strong energy dependence in the density of states coupled with the small Fermi energy. Similar measurements on LiC_6 produced a small, temperature-independent Knight shift. The observed negative frequency shift is attributed to core polarization of the Li^+Mu^- compound.

ACKNOWLEDGMENTS

Many helpful discussions with I. Affleck are gratefully acknowledged. One of the authors (J.A.C.) thanks S. Cox, K. Chow, and J. Brewer for numerous discussions related to muonium in semiconductors and graphite. Work at the University of Pennsylvania was supported by the U.S. Department of Energy, Grant No. DOE DEFG02-98ER45701.

[1] J.P. van Dyke, J. Nucl. Mater. **67–70**, 533 (1978).
[2] N.F. Lane and R.C. Cloney, J. Nucl. Mater. **67–70**, 582 (1978).
[3] Z.P. Popovic and M.J. Scott, Phys. Rev. B **5**, 2109 (1972).
[4] E. Zaremba, L.M. Sander, H.B. Shore, and J.H. Rose, J. Phys. F: Met. Phys. **7**, 1763 (1977).
[5] P. Jena and K.S. Singwi, Phys. Rev. B **17**, 3518 (1978).
[6] C.O. Almbladh, U. von Barth, Z.D. Popovic, and M.L. Stott, Phys. Rev. B **14**, 2250 (1976).
[7] F. Guinea and F. Flores, J. Phys. C **13**, 4137 (1980).
[8] J.K. Norskov, Phys. Rev. B **20**, 446 (1979).
[9] K. H. Chow, B. Hitti, and R. F. Kiefl, in *Identification of Defects in Semiconductors*, edited by M. Stavola (Academic Press, New York, 1998), p. 137.
[10] C. Rizzuto, Rep. Prog. Phys. **37**, 147 (1974).
[11] G. Gruner, Adv. Phys. **23**, 941 (1974).
[12] A. C. Hewson, *The Kondo Problem to Heavy Fermions* (Cambridge University Press, Cambridge, 1993).
[13] P. Nozieres, J. Low Temp. Phys. **17**, 31 (1974).
[14] W.A. MacFarlane *et al.*, Phys. Rev. B **58**, 1004 (1998).
[15] A. Schenck, Helv. Phys. Acta **54**, 471 (1982).
[16] W.A. MacFarlane *et al.*, Hyperfine Interact. **105**, 77 (1997).
[17] K.H. Chow, R.F. Kiefl, B. Hitti, T.L. Estle, and R.L. Lichti, Phys. Rev. Lett. **84**, 2251 (2002).
[18] S. Estreicher and P.F. Meier, Phys. Rev. B **27**, 642 (1983).
[19] D.E. Eastman *et al.*, Phys. Lett. **55A**, 309 (1975).
[20] E. Gilberg, Phys. Status Solidi B **69**, 477 (1975).
[21] Y. Fukai *et al.*, Solid State Commun. **19** (1976).
[22] O. Hartman, Hyperfine Interact. **4**, 828 (1978).
[23] T.M.S. Johnston *et al.*, Hyperfine Interact. **106**, 71 (1997).
[24] O. Hartmann *et al.*, Hyperfine Interact. **4**, 828 (1978).
[25] R.L. Garwin, L.M. Ledermann, and M. Weinrich, Phys. Rev. **105**, 1415 (1957).
[26] F.N. Gygax, A. Hintermann, A. Schenck, W. Studer, and A.J. Van Der Wal, Hyperfine Interact. **15-19**, 383 (1983).
[27] S.F.J. Cox *et al.*, J. Phys.: Condens. Matter **13**, 2169 (2001).
[28] Tao Zheng, J.S. Xue, and J.R. Dahn, Chem. Mater. **8**, 389 (1996).
[29] J.R. Dahn, Tao Zheng, J.S. Xue, and Yinghu Liu, Science **270**, 590 (1995).
[30] J. Chakhalian *et al.*, Hyperfine Interact. **106**, 245 (1997).
[31] A. Schenck, *Muon Spin Rotation Spectroscopy: Principle and Applications in Solid State Physics* (Adam Hilger, Bristol, 1985), p. 128.
[32] Dake Yu *et al.*, Chem. Phys. **142**, 229 (1990).
[33] V.I. Mel'nikov, JETP Lett. **5**, 414 (1982).
[34] J. Korringa, Physica (Amsterdam) **XVI**, 601 (1950).
[35] J.C. Slonczewski and P.R. Weiss, Phys. Rev. **109**, 272 (1959).
[36] J.W. McClure, Phys. Rev. **108**, 612 (1957).
[37] J.W. McClure, Phys. Rev. **119**, 606 (1960).
[38] S.F.J. Cox and M.C.R. Symons, Chem. Phys. Lett. **126**, 516 (1986).
[39] M.S. Dresselhaus and G. Dresselhaus, Adv. Phys. **30**, 255 (1981).
[40] M. Manninen, Phys. Rev. B **27**, 53 (1983).
[41] N.A.W. Holzwarth, S. Rabii, and L.A. Girifalco, Phys. Rev. B **18**, 5190 (1978).
[42] K. Ichimura, E. Takamura, and M. Sano, Synth. Met. **40**, 355 (1991).
[43] R.F. Kiefl *et al.*, Phys. Rev. Lett. **60**, 224 (1988).